

5.07 Tbit/s/ λ Mode-Division Multiplexing Free-Space Optical Communication System

Yiming Li⁽¹⁾, Gil Fernandes⁽²⁾, David Benton⁽¹⁾, Antonin Billaud⁽³⁾, Marco Fernandes⁽²⁾,
Mohammed Patel⁽¹⁾, Fernando Guiomar⁽²⁾, Andrew Ellis⁽¹⁾,

⁽¹⁾ Aston Institute of Photonic Technologies, Aston University, Birmingham, B4 7ET, UK, liy70@aston.ac.uk

⁽²⁾ Instituto de Telecomunicações, University of Aveiro, Aveiro, 3810-193, Portugal,

⁽³⁾ Cailabs, 1 Rue Nicolas Joseph Cugnot, Rennes, 35000, France,

Abstract We demonstrate a single-wavelength mode-division multiplexing free-space optical communication system utilising 6 Hermite-Gaussian modes. By employing probabilistic-shaped 256-QAM signals at 80 GBaud, this system achieved a record-high line rate of 5.07 Tbit/s/ λ in free-space optical communications. ©2024 The Author(s)

Introduction

Free-space optical (FSO) communications is a promising technology for high-capacity wireless communications. Recently, 1 Tbit/s/ λ single-input single-output (SISO) FSO communication systems were demonstrated^{[1],[2]}. Constrained by the limited electrical bandwidth and the noise, this data rate is approaching the limit of optical communication systems^[3]. To further improve the single-wavelength capacity in FSO transmissions, mode-division multiplexing (MDM) technology is frequently discussed as a promising candidate^{[4]–[9]}. While single-input multiple-output (SIMO) MDM systems were primarily employed to combat turbulence^[9], multiple-input multiple-output (MIMO) MDM systems have shown their potential to further increase the data rate^{[4],[5]}.

However, the MDM systems were constrained by practical inter-mode crosstalk and inter-symbol interference (ISI). Therefore, considerable performance degradation was observed when compared with the SISO counterparts, resulting in limited symbol rate and constellation complexity^{[4],[5],[7]}. As a result, pure MDM FSO systems only quantified a slight improvement in aggregate line rate when compared with SISO FSO systems^{[4],[5]}. Although remarkable results were achieved by employing two sets of “concentric rings”, each comprising multiple orbital angular momentum (OAM) modes^[4], the achievable spatial density was constrained by the incomplete OAM mode basis. Moreover, it introduced drawbacks such as increased beam size, varying beam divergence across different “rings”, and added system complexity, which hindered practical implementation.

In this paper, we demonstrate a 6×6 MDM FSO communication system using the 6 lowest order Hermite-Gaussian (HG) modes (Fig. 1). By employing multi-plane light conversion (MPLC) devices and carefully calibrating the optical paths, the inter-mode crosstalk was suppressed to < -25 dB.

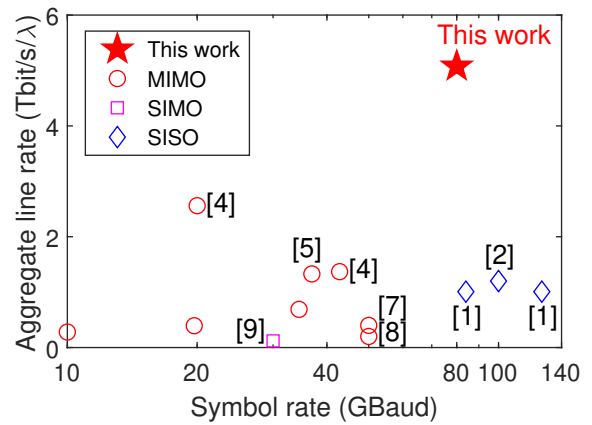


Fig. 1: The symbol rate and aggregate line rate of the state-of-the-art free-space optical communication systems.

By employing Volterra pre-distortion and careful mode-wise delay calibration, the intra- and inter-mode ISI were minimised, supporting a record-high 80 GBaud MDM transmission. By employing probabilistic shaping, the system achieved a record-high average mode-wise line rate of 845 Gbit/s/ λ in MDM FSO systems, leading to a record-high aggregate line rate of 5.07 Tbit/s/ λ in all FSO communication systems.

Methods and Experimental Setup

Our experimental MDM MIMO FSO communication system is depicted in Fig. 2. At the transmitter, a 1550.12 nm laser was modulated by a dual-polarisation (DP) in-phase and quadrature (IQ) modulator with a nominal 6 dB bandwidth of 45 GHz using a 4-channel 120 GSa/s arbitrary waveform generator (AWG) with a 3 dB bandwidth of 50 GHz, and a 80 GBaud signal was generated. The signal was root-raised cosine (RRC) shaped with a roll-off factor of 0.1 and pre-distorted by non-linear Volterra pre-distortion with kernel memory lengths of (201,9,9) taps^{[10],[11]}. The signal had a frame structure of 20,000 symbols with 1,920 quadrature phase-shift keying (QPSK) symbols in the training sequence, and 1 random QPSK

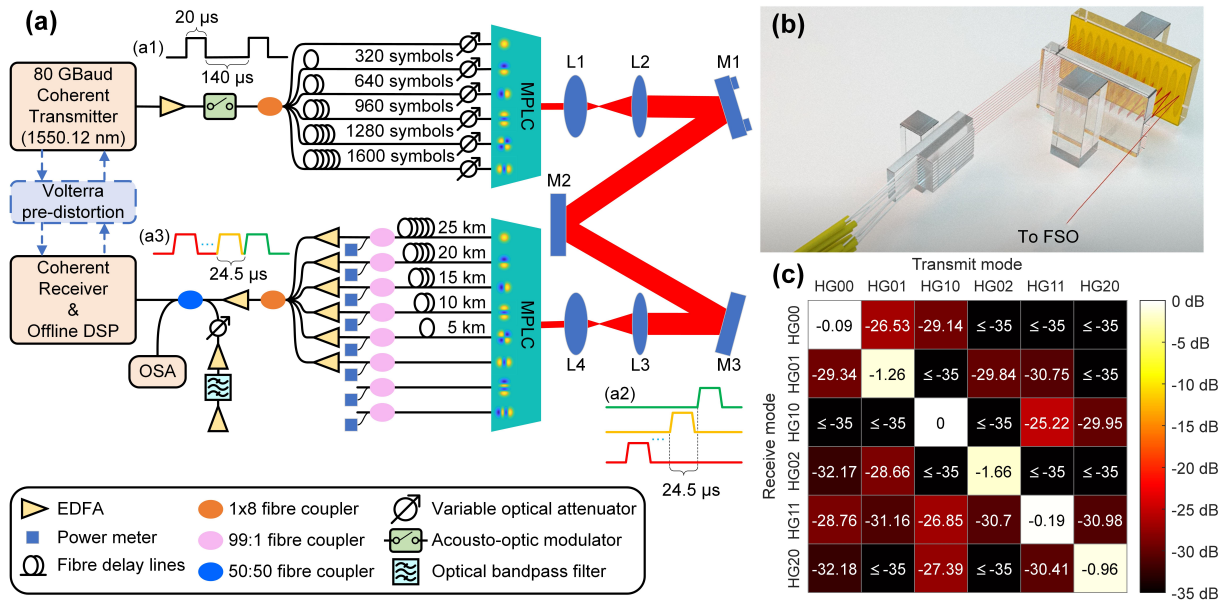


Fig. 2: Experimental setup for beaconless MDM communication system. L: lens; M: mirror; EDFA: erbium-doped fiber amplifier; MPLC: multi-plane light conversion; OSA: optical spectrum analyser; FSO: free-space optics. (a) Schematic diagram of experimental setup. (b) The structure of the MPLC device. (c) The normalised transfer matrix when the system is properly aligned.

pilot symbol for every 9 data symbols, the data symbols were either 16-QAM symbols generated from a $2^{15} - 1$ pseudo random binary sequence (PRBS) or PS-256-QAM symbols (shaping factor=2, constellation entropy ≈ 7.32) generated from a mt19937ar Mersenne Twister^[12]. After being amplified by an erbium-doped fiber amplifier (EDFA), the signals were passed through an acousto-optic modulator (AOM) to generate a $20 \mu\text{s}$ burst signal for each $160 \mu\text{s}$ period (Fig. 2(a1)) to enable the time-division multiplexing (TDM) receiver setup which will be detailed later. To emulate independent transmitters, 6 copies were split from the burst signal and delayed by precisely calibrated variable fibre delay lines (FDLs). These delay lengths were carefully set to 0, 320, 640, 960, 1280, and 1600 symbols with an error of less than 0.05 symbol. The delayed signals were passed through variable optical attenuators (VOAs) to compensate for practical power imbalances at the inputs of MPLC. The compensated signals were then converted to corresponding HG modes using MPLC technology (Fig. 2(b), the output beam waist diameter of the HG_{0,0} mode was $\sim 0.3 \text{ mm}$)^[13].

In the FSO channel, the transmitted HG modes were passed through a beam expander consisting of a convex lens with a focal length of 30 mm (L1) followed by another convex lens with a focal length of 100 mm (L2). The expanded beam was reflected off a steering mirror (M1) with two high-precision stepper-motor actuators for precise alignment. The beam was then reflected off two more mirrors (M2, M3), and another symmetric beam expander consisting of a convex lens with a focal length of 100 mm (L3) followed by another convex lens with a focal length of 30 mm (L4). The beam

was then coupled into the receiver MPLC device after a total FSO length of $\sim 1.6 \text{ m}$. Here we performed fine focal length matching by carefully adjusting L1-L4 towards the optical axis. Additionally, we ensured fine alignment by carefully adjusting M1 and M3. As shown in Fig. 2(c), the normalised transfer matrix achieved $< 1.7 \text{ dB}$ mode-dependent loss, and $> 25 \text{ dB}$ suppression for 6×6 MIMO when the system was optimally aligned.

At the receiver, the optical signals split by the receiver MPLC device were delayed by the FDLs for the 6 lowest order modes to realise the TDM receiver. A 5 km difference between adjacent modes introduced a $\sim 24.5 \mu\text{s}$ delay (Fig. 2(a2)), slightly longer than the signal burst (Fig. 2(a1)). Each delayed signal was then split by a 99:1 fibre coupler so that the overall power received by each mode could be measured by a corresponding power meter. Here, we also connected two more unused higher-order modes (i.e. HG_{0,3} and HG_{3,0}) to better observe the power leakage when aligning the FSO channel. The 6 lowest order modes were then amplified by 6 EDFAs, coupled into one single-mode fibre for TDM combining (Fig. 2(a3)), and amplified by another EDFA. Afterwards, the variable optical noise was loaded by a sequence of devices involving an EDFA, an optical bandpass filter, another EDFA, a VOA, and a 50:50 coupler. The average optical signal-to-noise ratio (OSNR) was then assessed using an optical spectrum analyser (OSA) to facilitate OSNR scanning. Finally, the TDM signals were received by a coherent receiver with a 70 GHz, 200 GSa/s oscilloscope and demodulated by an offline digital signal processing (DSP). The DSP includes a sequential combination of the Gram-

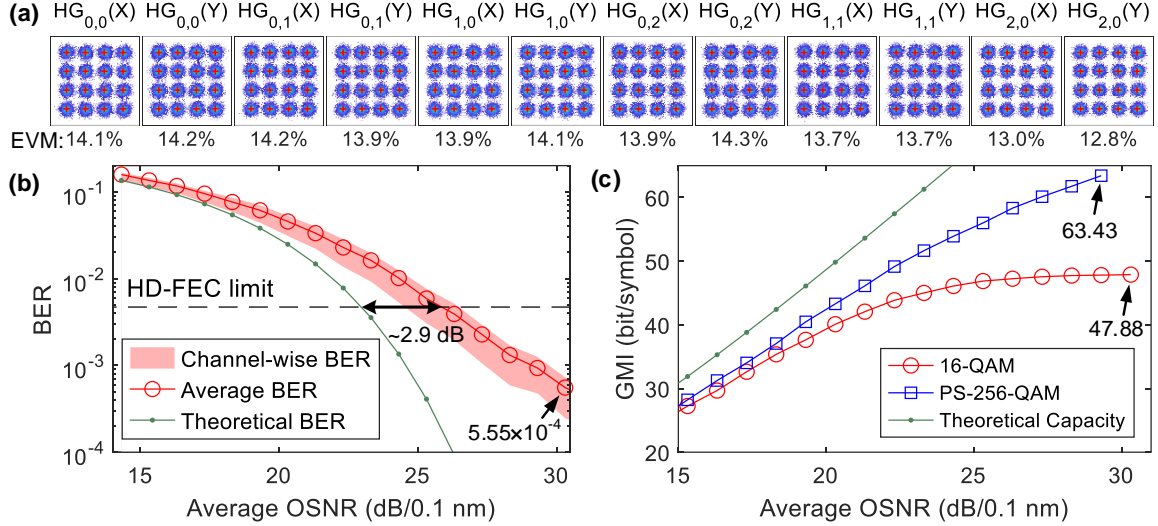


Fig. 3: Experimental results of the communication system. EVM: error vector magnitude; BER: bit error rate; OSNR: optical signal-to-noise ratio; HD-FEC: hard-decision forward error correction; GMI: generalized mutual information. (a) Constellation diagram. Red crosses: reference constellation points. (b) BER versus average OSNR for 16-QAM. (c) GMI versus average OSNR.

Schmidt orthogonalisation^[14], frequency-domain frequency offset estimation, frequency-domain chromatic dispersion (CD) compensation for the receiver FDLs^[15], Godard timing recovery^[16], phase-asynchronous phase and channel estimation^[17], and MIMO equalisation^[18].

Experimental Results

The experimental results are depicted in Fig. 3. Considering 16-QAM signals without noise loading, the channel-wise constellation diagrams are shown in Fig. 3(a). When the FSO system was optimally aligned, the error vector magnitude (EVM) performance across different channels was similar, with minor differences observed due to the mode-dependent loss in the MPLC devices.

Fig. 3(b) depicts the average bit error rate (BER) versus the average OSNR when loading 16-QAM signals. We observe an implementation penalty of <3 dB at the hard-decision forward error correction (HD-FEC) limit of 4.7×10^{-3} ^[19]. We believe this was mainly due to (1) the shot noise and quantisation noise in the coherent receiver; (2) the DSP implementation penalty; (3) the mode-dependent loss in the MPLC devices. To quantify the influence of mode-dependent loss, we illustrate the range of channel-wise BER with a shaded pink area in Fig. 3(b). We observed slight BER fluctuations between different channels, which was consistent with the EVM fluctuations in Fig. 3(a). In the high OSNR area, a minimum average BER of 5.55×10^{-4} was obtained, approximately an order of magnitude lower than the HD-FEC limit. As a result, an aggregate line rate of $80 \text{ GBaud} \times 6 \text{ modes} \times 2 \text{ polarisations} \times 4 \text{ bit/symbol} = 3.84 \text{ Tbit/s}$ was achieved when loading 16-QAM signals.

Fig. 3(c) depicts the aggregate generalized mutual information (GMI) versus the average OSNR

when loading 16-QAM signals and PS-256-QAM signals, respectively. In the low OSNR area, the experimental GMI aligned with the theoretical capacity, with approximately 1.13 dB and 1.56 dB OSNR degradation for PS-256-QAM signals and 16-QAM signals, respectively. We believe the 1.13 dB degradation mainly came from the DSP implementation penalty and the further 0.43 dB degradation for 16-QAM signals mainly came from the constellation penalty. In the high OSNR area, the 16-QAM signals achieved a GMI of 47.88 bit/symbol, approaching the theoretical limit of $6 \text{ modes} \times 2 \text{ polarisations} \times 4 \text{ bit/symbol} = 48 \text{ bit/symbol}$. When loading the PS-256-QAM signals, the GMI was further increased to 63.43 bit/symbol in the high OSNR area, while a higher deviation was observed from the theoretical capacity due to the practical implementation penalties. As a result, an aggregate line rate of $80 \text{ GBaud} \times 63.43 \text{ bit/symbol} = 5.07 \text{ Tbit/s}$ was achieved when loading PS-256-QAM signals.

Conclusions

In this paper, we have demonstrated a high symbol rate 6×6 HG-MDM FSO communication system. By employing MPLC-based mode-(de)multiplexer and precise alignment stages, the inter-mode crosstalk was suppressed to <-25 dB by careful beam alignment and optical path calibration. Moreover, the intra- and inter-mode ISI were minimised by employing Volterra pre-distortion and careful mode-wise delay calibration. As a result, our system supported up to 80 GBaud signals, achieving a line rate of $5.07 \text{ Tbit/s}/\lambda$ when loading PS-256-QAM signals and $3.84 \text{ Tbit/s}/\lambda$ when loading 16-QAM signals, respectively. These results indicated the feasibility of employing MDM technology for ultra-high capacity wireless communications.

Acknowledgements

We acknowledge the support by EPSRC under Grants EP/T009047/1, EP/S003436/1, and EP/S016171/1. This work was also partially supported by FEDER, through the CENTRO 2020 programme by FCT/MCTES through project OptWire (PTDC/EEI-TEL/2697/2021), by MSCA RISE programme through project DIOR (grant agreement no. 10100828), and by ORCIP (CENTRO-01-0145-FEDER-022141). Yiming Li acknowledges H2020-EU under the Marie Skłodowska-Curie Grant 713694. Gil M. Fernandes acknowledges funding by FCT through the individual scientific employment program (2022.07168.CEECIND).

References

- [1] B. I. Bitachon, Y. Horst, L. Kulmer, *et al.*, "Tbit/s single channel 53 km free-space optical transmission-assessing the feasibility of optical GEO-satellite feeder links", in *European Conference and Exhibition on Optical Communication*, Optica Publishing Group, 2022, Th3A–6.
- [2] M. A. Fernandes, P. P. Monteiro, and F. P. Guiomar, "Free-space terabit optical interconnects", *Journal of Lightwave Technology*, vol. 40, no. 5, pp. 1519–1526, 2022. DOI: 10.1109/JLT.2021.3133070.
- [3] D. Che, X. Chen, C. Deakin, and G. Raybon, "2.4-Tb/s single-wavelength coherent transmission enabled by 114-GHz all-electronic digital-band-interleaved DACs", in *49th European Conference on Optical Communications (ECOC 2023)*, IET, vol. 2023, 2023, pp. 1706–1709. DOI: 10.1049/icp.2023.2672.
- [4] J. Wang, J.-Y. Yang, I. M. Fazal, *et al.*, "Terabit free-space data transmission employing orbital angular momentum multiplexing", *Nature Photonics*, vol. 6, no. 7, pp. 488–496, 2012. DOI: 10.1038/nphoton.2012.138.
- [5] Z. Hu, Y. Li, D. M. Benton, A. A. Ali, M. Patel, and A. D. Ellis, "Single-wavelength transmission at 1.1-Tbit/s net data rate over a multi-modal free-space optical link using commercial devices", *Optics letters*, vol. 47, no. 14, pp. 3495–3498, 2022. DOI: 10.1364/OL.463941.
- [6] Y. Li, Z. Chen, D. M. Benton, M. Patel, M. P. Lavery, and A. D. Ellis, "Single-wavelength polarization-and mode-division multiplexing free-space optical communication at 689 Gbit/s in strong turbulent channels", *Optics Letters*, vol. 48, no. 13, pp. 3575–3578, 2023. DOI: 10.1364/OL.495334.
- [7] Y. Ren, Z. Wang, P. Liao, *et al.*, "Experimental characterization of a 400 Gbit/s orbital angular momentum multiplexed free-space optical link over 120 m", *Optics letters*, vol. 41, no. 3, pp. 622–625, 2016. DOI: 10.1364/OL.41.000622.
- [8] N. Hu, H. Song, R. Zhang, *et al.*, "Demonstration of turbulence mitigation in a 200-Gbit/s orbital-angular-momentum multiplexed free-space optical link using simple power measurements for determining the modal crosstalk matrix", *Optics Letters*, vol. 47, no. 14, pp. 3539–3542, 2022. DOI: 10.1364/OL.464217.
- [9] N. K. Fontaine, R. Ryf, Y. Zhang, *et al.*, "Digital turbulence compensation of free space optical link with multi-mode optical amplifier", in *45th European Conference on Optical Communication (ECOC 2019)*, IET, 2019, pp. 1–4. DOI: 10.1049/cp.2019.1015.
- [10] C. Eun and E. J. Powers, "A new Volterra predistorter based on the indirect learning architecture", *IEEE transactions on signal processing*, vol. 45, no. 1, pp. 223–227, 1997. DOI: 10.1109/78.552219.
- [11] M. Nölle, M. S. Erkiling, R. Emmerich, C. Schmidt-Langhorst, R. Elschner, and C. Schubert, "Characterization and linearization of high bandwidth integrated optical transmitter modules", in *2020 European Conference on Optical Communications (ECOC)*, IEEE, 2020, pp. 1–4. DOI: 10.1109/ECOC48923.2020.9333184.
- [12] M. Matsumoto and T. Nishimura, "Mersenne twister: a 623-dimensionally equidistributed uniform pseudo-random number generator", *ACM Transactions on Modeling and Computer Simulation (TOMACS)*, vol. 8, no. 1, pp. 3–30, 1998. DOI: 10.1145/272991.272995.
- [13] N. K. Fontaine, R. Ryf, H. Chen, D. T. Neilson, K. Kim, and J. Carpenter, "Laguerre-Gaussian mode sorter", *Nature communications*, vol. 10, no. 1, p. 1865, 2019. DOI: 10.1038/s41467-019-09840-4.
- [14] I. Fatadin, S. J. Savory, and D. Ives, "Compensation of quadrature imbalance in an optical QPSK coherent receiver", *IEEE Photonics Technology Letters*, vol. 20, no. 20, pp. 1733–1735, 2008. DOI: 10.1109/LPT.2008.2004630.
- [15] M. S. Faruk and S. J. Savory, "Digital signal processing for coherent transceivers employing multilevel formats", *Journal of Lightwave Technology*, vol. 35, no. 5, pp. 1125–1141, 2017. DOI: 10.1109/JLT.2017.2662319.
- [16] D. Godard, "Passband timing recovery in an all-digital modem receiver", *IEEE Transactions on Communications*, vol. 26, no. 5, pp. 517–523, 1978. DOI: 10.1109/TCOM.1978.1094107.
- [17] Y. Li, Z. Chen, M. Patel, M. P. Lavery, and A. D. Ellis, "Phase and channel estimation for high-capacity phase-asynchronous mode-division multiplexing multiple-input multiple-output free-space optical communications in strong turbulent channels", *Journal of Lightwave Technology*, 2024. DOI: 10.1109/JLT.2024.3375791.
- [18] S. Randel, R. Ryf, A. Sierra, *et al.*, "6 × 56-Gb/s mode-division multiplexed transmission over 33-km few-mode fiber enabled by 6 × 6 MIMO equalization", *Optics Express*, vol. 19, no. 17, pp. 16 697–16 707, 2011. DOI: 10.1364/OE.19.016697.
- [19] A. Alvarado, E. Agrell, D. Lavery, R. Maher, and P. Bayvel, "Replacing the soft-decision FEC limit paradigm in the design of optical communication systems", *Journal of Lightwave Technology*, vol. 33, no. 20, pp. 4338–4352, 2015. DOI: 10.1109/JLT.2015.2482718.